Published in final edited form as:
Cancer Res. 2010 April 15; 70(8): 3228–3238. doi:10.1158/0008-5472.CAN-09-4559.

Pharmacologic inhibition of cdk4/6 arrests the growth of glioblastoma multiforme intracranial xenografts

Karine Michaud[1,*], **David A. Solomon**[2,*], **Eric Oermann**[2], **Jung-Sik Kim**[2], **Wei-Zhu Zhong**[3], **Michael D. Prados**[1], **Tomoko Ozawa**[1], **C. David James**[1,†], and **Todd Waldman**[2,†]

[1]Department of Neurological Surgery, Helen Diller Comprehensive Cancer Center, University of California San Francisco, San Francisco, CA

[2]Department of Oncology, Lombardi Comprehensive Cancer Center, Georgetown University School of Medicine, Washington, DC

[3]Pfizer Oncology, La Jolla, CA

Abstract

Activation of cyclin-dependent kinases 4 and 6 (cdk4/6) occurs in the majority of glioblastoma multiforme (GBM) tumors, and represents a promising molecular target for the development of small molecule inhibitors. In the current study we investigated the molecular determinants and *in vivo* response of diverse GBM cell lines and xenografts to PD-0332991, a cdk4/6 specific inhibitor. *In vitro* testing of PD-0332991 against a panel of GBM cell lines revealed a potent G1 cell cycle arrest and induction of senescence in each of 16 Rb-proficient cell lines regardless of other genetic lesions, whereas each of 5 cell lines with homozygous inactivation of Rb were completely resistant to treatment. shRNA depletion of Rb expression conferred resistance of GBM cells to PD-0332991, further demonstrating a requirement of Rb for sensitivity to cdk4/6 inhibition. PD-0332991 was found to efficiently cross the blood-brain barrier and proved highly effective in suppressing the growth of intracranial GBM xenograft tumors, including those that had recurred after initial therapy with temozolomide. Remarkably, no mice receiving PD-0332991 had significant disease progression or died while on therapy. Additionally, the combination of PD-0332991 and radiation therapy resulted in significantly increased survival benefit compared with either therapy alone. In total, our results support clinical trial evaluation of PD-0332991 against newly-diagnosed as well as recurrent GBM, and indicate that Rb status is the primary determinant of potential benefit from this therapy.

Keywords

glioblastoma; cyclin-dependent kinase; Rb; $p16^{INK4a}$; PD-0332991; bioluminescence

Introduction

Deregulation of the cdk4/6-cyclin D-INK4-Rb signaling pathway is among the most common aberrations found in human cancer (1). In the case of glioblastoma multiforme

†Address correspondence to: Todd Waldman, MD, PhD, Associate Professor, Dept. Oncology, Lombardi Comprehensive Cancer Center, E304 Research Building, 3970 Reservoir Rd, N.W., Washington, DC 20057, Phone: 202-687-1340, waldmant@georgetown.edu, C. David James, PhD, Guggenhime Professor, Dept. Neurosurgery, Assoc. Director, Brain Tumor Res. Center, 1450 3rd Street, Room HD283, University of California, San Francisco, San Francisco, CA. 94143-0520, Phone: (415) 476-5876, david.james@ucsf.edu.
*Contributed equally to this report

(GBM), this pathway is most commonly altered by homozygous deletion of CDKN2A/B, and less commonly by deletion/mutation of CDKN2C and RB1, or genomic amplification of CDK4, CDK6, and individual D-type cyclins (2–8). Recent molecular profiling of GBM has further highlighted the critical role of cdk4/6 activation in the pathogenesis of this devastating tumor (9,10).

Despite the ubiquitous nature of cdk4/6 activation in human cancer, surprisingly little work has been reported describing efforts to target activated cdk4/6 with pharmacological inhibitors. This is due to the difficulty of identifying inhibitors specific to cdk4/6, and also because cdk inhibition is predicted to be cytostatic (not cytotoxic), and therefore of uncertain therapeutic utility (11).

PD-0332991 is a recently developed cdk4/6 specific inhibitor. Initial reports detailed the synthesis of this pyridopyrimidine derivative, demonstrated its *in vitro* specificity against cdk4/6, and documented its potent anti-proliferative activity against Rb-proficient subcutaneous human tumor xenografts (12,13). A large phase I study of this compound is ongoing and has already demonstrated clinical efficacy against otherwise untreatable teratomas (14). Additional xenograft studies modeling disseminated multiple myeloma (15) and breast carcinoma (16) helped to motivate recently initiated phase I/II clinical trials testing PD-0332991 against these cancers (http://www.clinicaltrials.gov).

Given its effectiveness in a variety of tumor types and its specificity for activated cdk4/6, we hypothesized that PD-0332991 could be useful in the treatment of GBM. To evaluate this, PD-0332991 was initially tested *in vitro* against a panel of 21 human GBM cell lines of defined genetic backgrounds. Next, its activity was assayed *in vivo* against three different GBM intracranial xenografts using a luciferase reporter to allow longitudinal monitoring of tumor growth and response to therapy. Finally, PD-0332991 was tested in combination with ionizing radiation against intracranial xenografts, as well as in tumors that had recurred following initial therapy with temozolomide, an alkylating agent routinely used in upfront treatment of GBM (17). Our findings demonstrate that PD-0332991 crosses the blood-brain barrier and works effectively both as a single agent and in combination with radiation to suppress the growth of all Rb-proficient GBM cells and tumors tested.

Materials and Methods

GBM cell lines and xenografts

A panel of 21 GBM cell lines was obtained directly from the American Type Culture Collection (U87MG, U138MG, M059J, Hs683, H4, A172, LN18, LN229, CCF-STTG1, T98G, and DBTRG-05MG), DSMZ (8MGBA, 42MGBA, DKMG, GAMG, GMS10, LN405, and SNB19), and the Japan Health Sciences Foundation Health Science Research Resources Bank (AM38, NMC-G1, and KG-1-C). These repositories authenticate all human cell lines prior to accession by DNA fingerprinting, and independent evidence of authenticity is also provided by cytogenetic and immunophenotypic tests. All experiments were performed on cell lines that had been passaged for less than six months after receipt. Cell line SF767 was established from a GBM at the UCSF Brain Tumor Research Center, and has been previously genotyped for CDKN2A, TP53, and PTEN status (18). All cell lines were grown in DMEM + 10% fetal bovine serum at 37°C in 5% CO_2. GBM 39 is a human GBM primary xenograft maintained as a subcutaneous heterotransplant in athymic mice, as previously described (19).

Western blot

Total cell lysate was collected from asynchronously proliferating cells in RIPA buffer, resolved by SDS-PAGE, and then immunoblotted using standard techniques. Primary

antibodies used were obtained from Santa Cruz Biotechnology (Mdm2, clone SMP14), Cell Signaling (cyclin D1, clone DCS6; cyclin D3, clone DCS22; cdk4, clone DCS156; cdk6, clone DCS83; p18INK4c, clone DCS118; p21WAF1/CIP1, clone DCS60; p14ARF, clone 4C6/4; Rb, clone 4H1), BD PharMingen (p16INK4a, #554079), NeoMarkers (α-tubulin, Ab-1 clone DM1A; EGFR, Ab-12), CalBiochem (p53, Ab-6 clone DO-1), and Cascade Bioscience (PTEN, clone 6H2.1).

Flow cytometry

Cells were pulsed with 10 μmol/L bromodeoxyuridine (BrdU) for 1 h, trypsinized, and centrifuged. Cells were fixed and stained using the BrdU Flow kit (Pharmingen), counterstained with propidium iodide, and analyzed by flow cytometry in a BD FACSort instrument using FCS Express v.3 software (DeNovo Software).

β-Galactosidase staining

Cells grown on coverslips were stained with the Senescence β-Galactosidase Staining kit (Cell Signaling) as described by the manufacturer.

Microscopy

Imaging was performed on an Olympus BX61 light microscope with Plan-Apochromat objectives.

Rb knockdown

Five unique shRNAs to the RB1 mRNA in the pLKO.1-Puro lentiviral expression vector were obtained from Open Biosystems. To make virus, empty pLKO.1-Puro or each of these 5 shRNA clones were cotransfected into 293T cells with pVSV-G (Addgene) and pHR'-CMV-8.2ΔR (Addgene) helper plasmids using Fugene 6 (Roche). Virus-containing conditioned medium was harvested 48 h after transfection, filtered, and used to infect recipient cells in the presence of 8 μg/mL polybrene. Infected cells were selected with 2 μg/mL puromycin until all mock-infected cells were dead and then maintained in 0.2 μg/mL puromycin.

Generation and therapy of mice with intracranial GBM xenograft tumors

All intracranial therapy response experiments involved the use of 5–6 week-old female athymic mice (nu/nu genotype, BALB/c background, Simonsen Laboratories). Animals were housed and fed under aseptic conditions, and all animal research was approved by The University of California, San Francisco Institutional Animal Care and Use Committee. Procedures used for intracranial tumor establishment, including monitoring of tumor growth and response to therapy by bioluminescence imaging, have previously been described (20). Treatments for the experiments reported here were as follows: oral administration of vehicle only for control groups (50 mM sodium lactate, pH 4, for PD-0332991, and/or OraPlus for temozolomide), oral administration of PD-0332991 (Pfizer) at 150 mg/kg/day, clinical-grade temozolomide (Schering-Plough) at 10 mg/kg/day, and radiation at 2 Gy/day from a Cesium-137 source (J. L. Shepherd & Associates).

Brain tumor analysis

PD-0332991 concentrations in mouse brain or brain tumor were determined using an LC-MS/MS method following liquid-liquid extraction (LLE). Brain or brain tumor samples were homogenized with purified water at 1:4 dilution (w/v). A 100 μL aliquot of the homogenate was used for LLE with the addition of 100 μL of potassium bicarbonate buffer, 10 μL of the stable labeled internal standard (IS), and 0.4 mL methyl tert-butyl ether. Following centrifugation, the organic layer was evaporated to dryness and reconstituted in

100 μL of methanol for LC-MS/MS analysis. The LC system (Shumadzu) was coupled to an MDS Sciex API 4000 triple quadrupole mass spectrometer, and operated in the positive ionization mode using multiple reaction source. PD-0332991 and IS were monitored using specific precursor ion → product ion transitions of *m/z* 448 → 380 and *m/z* 451 → 383, respectively. The final concentration of PD-0332991 was normalized based on the weight of mouse brain or brain tumor collected.

Results

Ubiquitous genetic lesions of the cdk4/6-cyclin D-INK4-Rb signaling pathway in GBM cell lines

Copy number and sequencing data from our previous analyses (7,21,22) and from the Cancer Genome Project of the Wellcome Trust Sanger Institute (http://www.sanger.ac.uk/genetics/CGP) were analyzed to identify the genetic status of the major known GBM oncogenes and tumor suppressor genes in a panel of 21 GBM cell lines. This analysis demonstrated genetic lesions in at least one component of the cdk4/6-cyclin D-INK4-Rb signaling pathway in each cell line, without exception (Table 1). Fifteen of the cell lines have homozygous deletion of CDKN2A and CDKN2B, five have homozygous deletion or mutation of RB1 (resulting in a lack of detectable Rb protein), four have homozygous deletion of CDKN2C, and one (CCF-STTG1) harbors amplifications of both CDK6 and CCND3, with high levels of expression of corresponding encoded proteins (Table 1 and Supplemental Fig. S1). Lesions of CDKN2A/B, RB1, and CDK6/CCND3 were mutually exclusive in these 21 cell lines, except for 42MGBA cells which harbor homozygous deletion of CDKN2A/B and express no detectable Rb protein. In contrast, homozygous deletion of CDKN2C occurred exclusively in cell lines also harboring homozygous deletions of CDKN2A/B. A number of additional genetic lesions in other signaling pathways were identified among the cell lines, including PTEN deletion and mutation, TP53 mutation, BRAF mutation, EGFR rearrangement, and MDM2 amplification (Supplemental Table S1). However, no concordance was detected between any of these other genetic lesions and lesions of cdk4/6-cyclin D-INK4-Rb signaling pathway genes.

PD-0332991 induces cell cycle arrest and senescence of Rb-proficient GBM cells

Each of the 21 GBM cell lines was cultured *in vitro* in the presence of either 1 μM PD-0332991 or vehicle alone. At 48 hours post-treatment, cell cycle distribution was assessed by BrdU incorporation and flow cytometry analysis (Fig. 1*A–B* and Supplemental Fig. S2). In 16/21 cell lines PD-0332991 treatment significantly inhibited BrdU incorporation and resulted in an increased fraction of cells in G1 phase of the cell cycle compared to vehicle alone (Table 1). While some cell lines displayed a greater than 95% reduction in BrdU incorporation after treatment with 1 μM PD-0332991 for 48 hrs (*e.g.* A172, CCF-STTG1, DBTRG-05MG, DKMG, Hs683, KG-1-C, NMC-G1, SNB19, U87MG), others displayed a more intermediate response (*e.g.* AM38, GAMG, H4, LN18). Of note, 5/21 of the cell lines displayed no difference in cell cycle distribution between treatment with vehicle or 1 μM PD-0332991 (8MGBA, 42MGBA, GMS10, LN405, and M059J). Remarkably, each of the five resistant cell lines harbors homozygous deletion or mutation of the RB1 gene that result in the absence of detectable Rb protein (see Supplemental Fig. S1).

To further explore the differential sensitivity of GBM cell lines to PD-0332991, the 21 cell lines were next cultured in the presence of 0, 1, 2, or 10 μM PD-0332991, and cell cycle distribution was again assessed at 48 hrs post-treatment (Supplemental Fig. S3). Cells that initially displayed >95% reduction in BrdU incorporation at 1 μM demonstrated similar inhibition at doses of 2 and 10 μM PD-0332991, and without evidence of apoptosis or

cytotoxicity (*i.e.*, floating cell debris or sub-G1 DNA content) at any dose (data not shown). Importantly, Rb-proficient cells that displayed intermediate reductions in BrdU incorporation at 1 μM PD-0332991 displayed increased reductions when incubated with 2 and 10 μM PD-0332991. For example, GAMG cells displayed a 53% reduction in BrdU incorporation at 1 μM PD-0332991, but had 78% and 96% reductions at 2 and 10 μM, respectively. In contrast, the five Rb-deficient cell lines displayed no reduction in BrdU incorporation or alterations in cell cycle distribution at any of the doses tested.

We next examined the effects of long-term culture in the presence of PD-0332991. Microscopic analysis of Rb-proficient GBM cells treated with 1 μM PD-0332991 for 7 days revealed not only sustained growth arrest, but also morphological changes characteristic of cells that have exited the cell cycle and entered a senescent-like state (*i.e.*, large and flat: Fig. 1*C*). Senescence-associated β-galactosidase activity was evident in RB-proficient GBM cells after 14 days of treatment with PD-0332991 (Fig. 1*D*). However, Rb-deficient cells did not display these morphologic and senescent-like changes (Fig. 1*C–D*). Together, these findings indicate that PD-0332991 potently induces G1 cell cycle arrest of GBM cells at doses of <1 to 10 μM, and that sustained treatment induces cellular senescence in Rb-proficient cells.

Stable depletion of Rb expression alleviates the growth arrest induced by PD-0332991

To unequivocally determine if Rb status dictates the sensitivity of GBM cells to PD-0332991, U87MG cells were infected with lentiviruses expressing five unique shRNAs to RB1, and stably-expressing clones were generated by puromycin selection. Two of the clones (19 and 63) demonstrated greater than 99% knockdown of Rb expression relative to cells infected with the pLKO.1 vector alone (Fig. 2*A*). BrdU incorporation and flow cytometry analysis at 48 hrs post-treatment revealed that Rb knockdown had substantially mitigated the cell cycle inhibitory effects of PD-0332991 in clones 19 and 63, relative to the empty vector pLKO.1 clone (Fig. 2*B*). Long-term culture of clones 19 and 63 with 1 μM PD-0332991 demonstrated their failure to arrest in the presence of drug, resulting in eventual growth to confluence (Fig. 2*C*), albeit at a slower rate than cells treated with vehicle alone.

PD-0332991 suppresses the growth of GBM intracranial xenografts

Next we tested whether orally-administered PD-0332991 could efficiently cross the blood-brain barrier and effectively suppress the growth of intracranial GBM tumors comprised of cells with known sensitivity *in vitro*. To do this, we established luciferase-modified U87MG xenografts in the brains of a series of athymic mice, with half receiving daily PD-0332991 by oral gavage, and the other half receiving vehicle only. Bioluminescence monitoring showed sustained anti-proliferative activity of PD-0332991 throughout the four-week course of treatment (Fig. 3*A left panel*), with tumor growth only evident upon completion of therapy. Consistent with these results, the survival of PD-0332991 treated mice was significantly extended relative to mice receiving vehicle only (Fig. 3*A right panel*, Supplemental Table 2). Importantly, none of the mice receiving PD-0332991 succumbed to tumor-related death while on therapy. In contrast, intracranial xenografts derived from the Rb-deficient cell line SF767 were completely resistant to PD-0332991 treatment (Supplemental Fig. S4).

To provide formal proof that PD-0332991 crosses the blood-brain barrier, we dissected the brain of a mouse and measured the levels of PD-0332991 in the U87MG xenograft tumor, in surrounding normal brain, and in brain from contralateral hemisphere. Notably, LC-MS/MS analysis revealed the presence of PD-0332991 in all three intracranial tissues. Furthermore, the drug was present at a 25–35× higher concentration in tumor tissue than in normal tissue

(Fig. 3*B*). Next, the brains from treated and untreated mice with intracranial U87MG tumors (matched with respect to their time of sacrifice) were formalin fixed, embedded in paraffin, and sectioned for MIB-1 immunohistochemistry. Treatment with PD-0332991 led to a greater than 8-fold reduction in MIB-1 index (Fig. 3*C*).

It is widely appreciated that established GBM cell lines do not recapitulate several aspects of GBM biology (*e.g. in vivo* invasiveness, the presence of genomic amplifications, gene expression profiles [19,22–24]). Therefore, we next tested the efficacy of PD-0332991 against a model system that has been shown to preserve patient tumor characteristics that are lost and/or suppressed with extended *in vitro* propagation – primary intracranial xenografts generated from surgically resected human tissue that have been directly implanted and serially passaged in nude mice (19). To do this, mice harboring primary intracranial xenografts of luciferase-modified GBM 39 (which harbors a homozygous deletion of the CDKN2A/B locus and is Rb-proficient [25]) were randomized to control and treatment groups at 25 days post injection of tumor cells. Daily treatment with PD-0332991 resulted in sustained growth suppression (Fig. 3*D left panel*), with significant survival benefit to treatment group mice (Fig. 3*D right panel*, Supplemental Table 2).

PD-0332991 combined with radiation therapy enhances survival of mice with GBM intracranial xenografts

Radiation has long been used as standard of care for treating newly-diagnosed GBM following surgical debulking of tumor (26), and investigational drugs for treating newly-diagnosed GBM are likely to see use with radiotherapy. To assess combined effects of radiation and PD-0332991 therapy, we established U87MG intracranial tumors in the brains of athymic mice and randomized them to four treatment groups at day 13 post-injection of tumor cells: control (mock treated), radiotherapy only (2 Gy/day, days 13–17), PD-0332991 only (150mg/kg/day, days 13–26), or combination therapy with radiation administered either concurrently (RTc) or sequentially (RTs), with PD-0332991 and radiation combination regimens dosed identically to their corresponding monotherapy regimens. Both bioluminescence and survival analysis showed that anti-tumor activity was most pronounced for mice receiving combination therapy, either concurrent or sequential (Fig. 4*A*–*B*, Supplemental Table 2).

PD-0332991 effectively suppresses the growth of recurrent GBM

An additional clinical scenario that often provides a setting for initial testing of an investigational agent is the treatment of recurrent cancer. For modeling this situation, mice with intracranial U87MG tumors were treated with 10 mg/kg/day temozolomide for 5 consecutive days, and subsequently monitored for initial anti-tumor activity of therapy, as well as for tumor regrowth from therapy (Fig. 5*A*). At time of tumor regrowth, mice were randomized to four treatment groups: (i) no additional treatment, (ii) repeat treatment with the same temozolomide regimen, (iii) treatment with PD-0332991 at 150 mg/kg/day for 2 weeks, or (iv) combined treatment with temozolomide and PD-0332991 administered concurrently at identical doses as the monotherapies. Both bioluminescence monitoring (Fig. 5*B*) and survival analysis (Fig. 5*C*, Supplemental Table 2) indicated that each therapy resulted in improved survival compared to no additional treatment. Furthermore, there was a trend favoring combination therapy with temozolomide and PD-0332991 as the most efficacious.

Discussion

Frequent and perhaps obligatory genetic alteration affecting the cdk4/6-cyclin D-INK4-Rb growth regulatory axis in GBM is well documented (2–8; Table 1 in the current report), and

has been recently corroborated in two large-scale, multi-institutional genomic analyses of GBM (9,10). The most common alteration of this pathway in GBM is homozygous deletion of CDKN2A/B, encoding $p16^{INK4a}$ and $p15^{INK4b}$, present in greater than 50% of tumors. Other alterations include amplification and overexpression of CDK4 (15–20%) and homozygous deletion/mutation of RB1 (~10%). Amplification of CDK6 and individual D-type cyclins, and homozygous deletion of CDKN2C encoding $p18^{INK4c}$ are less common. Of these alterations, only genetic inactivation of RB1 itself is thought to render a tumor resistant to inhibition of cdk4/6. Since genetic inactivation of RB1 occurs infrequently in GBM, a substantial majority of GBM patients are predicted to be candidates for therapies targeting cdk4/6.

Several previous studies have tested the effects of kinase inhibitors against GBM (*e.g.* imatinib, erlotinib, flavopiridol), both in a preclinical setting and in clinical trials without significant efficacy (27–29). While some of these compounds promiscuously inhibit cyclin-dependent kinases (*e.g.* flavopiridol), none of the previously tested compounds display selectivity for cyclin-dependent kinases relative to other kinases that may or may not be activated in GBM. Our study for the first time tests a cdk-specific inhibitor in the treatment of GBM, demonstrating significant efficacy both *in vitro* and *in vivo* as a single agent and in combination with radiation therapy.

PD-0332991 is an orally available pyridopyrimidine derivative that selectively inhibits cyclin-dependent kinases 4 and 6 (12), leading to a reduction in Rb phosphorylation and subsequent cell cycle arrest. The *in vitro* and *in vivo* results presented here further emphasize that Rb is the primary determinant of sensitivity to cdk4/6 inhibition. This aspect of PD-0332991 efficacy should be especially attractive with respect to clinical trial evaluation, since there are excellent reagents and protocols established for immunohistochemical detection of Rb in paraffin-embedded tissues (14,30).

Though Rb expression is clearly the primary determinant of tumor cell response to PD-0332991, variable growth inhibition among Rb-proficient cell lines (Table 1) suggests the existence of secondary factors that influence tumor cell sensitivity to PD-0332991, such as tumor CDK4/6 amplification vs. CDKN2A homozygous deletion. For the cell lines examined here, the single case with CDK6 amplification (CCF-STTG1) showed substantial sensitivity to PD-0332991 (Table 1).

Analysis of GBM response to PD-0332991 *in vivo*, using three different GBM tumor cell sources for establishing intracranial tumors (Fig. 3), yielded results entirely consistent with the *in vitro* data. PD-0332991 arrested the growth of xenografts generated from U87MG cells and GBM 39 (both Rb-proficient) and led to significantly improved survival (Fig. 3). The growth inhibitory effect of PD-0332991 was remarkably durable during the period of treatment.

Recent studies point to interest in investigating anti-tumor effects of PD-0332991 in combination with therapeutics that affect tumor properties other than cell cycling. For instance, it has been shown that PD-0332991, which by itself does not promote apoptotic response of cancer cells, markedly enhances myeloma cell killing by dexamethasone (31) as well as by bortezomib (32). Similarly, PD-0332991 has been shown to enhance breast cancer cell sensitivity to tamoxifen *in vitro* (33). Here, our bioluminescence and survival analysis of mice with intracranial U87MG tumors indicate that the anti-tumor activity of PD-0332991 when used with radiation, either concurrently or sequentially, is superior to using either agent as a monotherapy (Fig. 4). These results, therefore, could help motivate clinical trial testing of PD-0332991 against newly-diagnosed GBM, for which the use of radiotherapy is the standard of care.

Finally, treatment of intracranial GBM tumors that had re-grown following initial therapy with temozolomide demonstrated that PD-0332991 has activity against recurrent GBM (Fig. 5). These results additionally suggest a general approach for pre-clinical animal model testing of therapies for patients with recurrent brain tumors, which is a mostly neglected area of neurooncology research.

In total, these findings provide strong support for evaluating the efficacy of PD-0332991 in treating GBM patients. For future investigation, it will be interesting to examine combination therapies involving PD-0332991 with small molecule inhibitors targeting activated gene products in other GBM core pathways, such as erlotinib for inhibiting EGFR. Determination of the full range of applications of this cdk4/6 inhibitor will undoubtedly prove informative, and will hopefully lead to improved treatment for this devastating cancer.

Supplementary Material

Refer to Web version on PubMed Central for supplementary material.

Acknowledgments

We thank Karen Creswell and Annie Park for assistance with flow cytometry, Raquel Santos for assistance in conducting the intracranial xenograft therapy response experiments, Minerva Batugo for assistance with the LC-MS/MS analysis of brain tumor samples, and Michael Pishvaian and Erik Knudsen for helpful discussions.

Supported by NIH grants CA097257 (KM, TO, CDJ), CA115699 (TW), and American Cancer Society grant RSG0619101MGO (TW).

References

1. Malumbres M, Barbacid M. Cell cycle, CDKs and cancer: a changing paradigm. Nature Rev Cancer 2009;9:153–166. [PubMed: 19238148]
2. Jen J, Harper JW, Bigner SH, et al. Deletion of p16 and p15 genes in brain tumors. Cancer Res 1994;54:6353–6358. [PubMed: 7987828]
3. He J, Allen JR, Collins VP, et al. CDK4 amplification is an alternative mechanism to p16 gene homozygous deletion in glioma cell lines. Cancer Res 1994;54:5804–5807. [PubMed: 7954404]
4. He J, Olson JJ, James CD. Lack of p16INK4 or retinoblastoma protein (pRb), or amplification-associated overexpression of cdk4 is observed in distinct subsets of malignant glial tumors and cell lines. Cancer Res 1995;55:4833–4836. [PubMed: 7585516]
5. Ichimura K, Schmidt EE, Goike HM, Collins VP. Human glioblastomas with no alterations of the CDKN2A (p16INK4A, MTS1) and CDK4 genes have frequent mutations of the retinoblastoma gene. Oncogene 1996;13:1065–1072. [PubMed: 8806696]
6. Ueki K, Ono Y, Henson JW, Efird JT, von Deimling A, Louis DN. CDKN2/p16 or RB alterations occur in the majority of glioblastomas and are inversely correlated. Cancer Res 1996;56:150–153. [PubMed: 8548755]
7. Solomon DA, Kim JS, Jenkins S, et al. Identification of p18INK4c as a tumor suppressor gene in glioblastoma multiforme. Cancer Res 2008;68:2564–2569. [PubMed: 18381405]
8. Wiedemeyer R, Brennan C, Heffernan TP, et al. Feedback circuit among INK4 tumor suppressors constrains human glioblastoma development. Cancer Cell 2008;13:355–364. [PubMed: 18394558]
9. The Cancer Genome Atlas Network. Comprehensive genomic characterization defines human glioblastoma genes and core pathways. Nature 2008;455:1061–1068. [PubMed: 18772890]
10. Parsons DW, Jones S, Zhang X, et al. An integrated genomic analysis of human glioblastoma multiforme. Science 2008;321:1807–1812. [PubMed: 18772396]
11. Lapenna S, Giordano A. Cell cycle kinases as therapeutic targets for cancer. Nature Rev Drug Disc 2009;8:547–566.
12. Toogood PL, Harvey PJ, Repine JT, et al. Discovery of a potent and selective inhibitor of cyclin-dependent kinase 4/6. J Med Chem 2005;48:2388–2406. [PubMed: 15801831]

13. Fry DW, Harvey PJ, Keller PR, et al. Specific inhibition of cyclin-dependent kinase 4/6 by PD 0332991 and associated antitumor activity in human tumor xenografts. Mol Cancer Ther 2004;3:1427–1438. [PubMed: 15542782]
14. Vaughn DJ, Flaherty K, Lal P, et al. Treatment of growing teratoma syndrome. N Engl J Med 2009;360:423–424. [PubMed: 19164198]
15. Baughn LB, Di Liberto M, Wu K, et al. A novel orally active small molecule potently induces G1 arrest in primary myeloma cells and prevents tumor growth by specific inhibition of cyclin-dependent kinase 4/6. Cancer Res 2006;66:7661–7667. [PubMed: 16885367]
16. Zhang C, Yan Z, Arango ME, Painter CL, Anderes K. Advancing bioluminescence imaging technology for the evaluation of anticancer agents in the MDA-MB-435-HAL-Luc mammary fat pad and subrenal capsule tumor models. Clin Cancer Res 2009;15:238–246. [PubMed: 19118051]
17. Villano JL, Seery TE, Bressler LR. Temozolomide in malignant gliomas: current use and future targets. Cancer Chemother Pharmacol 2009;64:647–655. [PubMed: 19543728]
18. Ishii N, Maier D, Merlo A, et al. Frequent co-alterations of TP53, p16/CDKN2A, p14ARF, PTEN tumor suppressor genes in human glioma cell lines. Brain Pathol 1999;9:469–479. [PubMed: 10416987]
19. Giannini C, Sarkaria JN, Saito A, et al. Patient tumor EGFR and PDGFRA gene amplifications retained in an invasive intracranial xenograft model of glioblastoma multiforme. Neuro Oncol 2005;7:164–176. [PubMed: 15831234]
20. Sarkaria JN, Yang L, Grogan PT, et al. Identification of molecular characteristics correlated with glioblastoma sensitivity to EGFR kinase inhibition through use of an intracranial xenograft test panel. Mol Cancer Ther 2007;6:1167–1174. [PubMed: 17363510]
21. Solomon DA, Kim JS, Cronin JC, et al. Mutational inactivation of PTPRD in glioblastoma multiforme and malignant melanoma. Cancer Res 2008;68:10300–10306. [PubMed: 19074898]
22. Solomon DA, Kim JS, Ressom HW, et al. Sample type bias in the analysis of cancer genomes. Cancer Res 2009;69:5630–5633. [PubMed: 19567670]
23. Bigner SH, Humphrey PA, Wong AJ, et al. Characterization of the epidermal growth factor receptor in human glioma cell lines and xenografts. Cancer Res 1990;50:8017–8022. [PubMed: 2253244]
24. Camphausen K, Purow B, Sproull M, et al. Influence of in vivo growth on human glioma cell line gene expression: convergent profiles under orthotopic conditions. Proc Natl Acad Sci USA 2005;102:8287–8292. [PubMed: 15928080]
25. Hodgson JG, Yeh RF, Ray A, et al. Comparative analyses of gene copy number and mRNA expression in glioblastoma multiforme tumors and xenografts. Neuro Oncol 2009;11:477–487. [PubMed: 19139420]
26. Chang JE, Khuntia D, Robins HI, Mehta MP. Radiotherapy and radiosensitizers in the treatment of glioblastoma multiforme. Clin Adv Hematol Oncol 2007;5(894–902):907–915.
27. Reardon DA, Dresemann G, Taillibert S, et al. Multicentre phase II studies evaluating imatinib plus hydroxyurea in patients with progressive glioblastoma. Br J Cancer. 2009 Epub Nov 10.
28. Mellinghoff IK, Wang MY, Vivanco I, et al. Molecular determinants of the response of glioblastomas to EGFR kinase inhibitors. N Engl J Med 2005;353:2012–2024. [PubMed: 16282176]
29. Alonso M, Tamasdan C, Miller DC, Newcomb EW. Flavopiridol induces apoptosis in glioma cell lines independent of retinoblastoma and p53 tumor suppressor pathway alterations by a caspase-independent pathway. Mol Cancer Ther 2003;2:139–150. [PubMed: 12589031]
30. Burns KL, Ueki K, Jhung SL, Koh J, Louis DN. Molecular genetic correlates of p16, cdk4, and pRb immunohistochemistry in glioblastomas. J Neuropathol Exp Neurol 1998;57:122–130. [PubMed: 9600204]
31. Baughn LB, Di Liberto M, Wu K, et al. A novel orally active small molecule potently induces G1 arrest in primary myeloma cells and prevents tumor growth by specific inhibition of cyclin-dependent kinase 4/6. Cancer Res 2006;66:7661–7667. [PubMed: 16885367]
32. Menu E, Garcia J, Huang X, et al. A novel therapeutic combination using PD 0332991 and bortezomib: study in the 5T33MM myeloma model. Cancer Res 2008;68:5519–5523. [PubMed: 18632601]

33. Finn RS, Dering J, Conklin D, et al. PD 0332991, a selective cyclin D kinase 4/6 inhibitor, preferentially inhibits proliferation of luminal estrogen receptor-positive human breast cancer cell lines in vitro. Breast Cancer Res 2009;11:R77. [PubMed: 19874578]

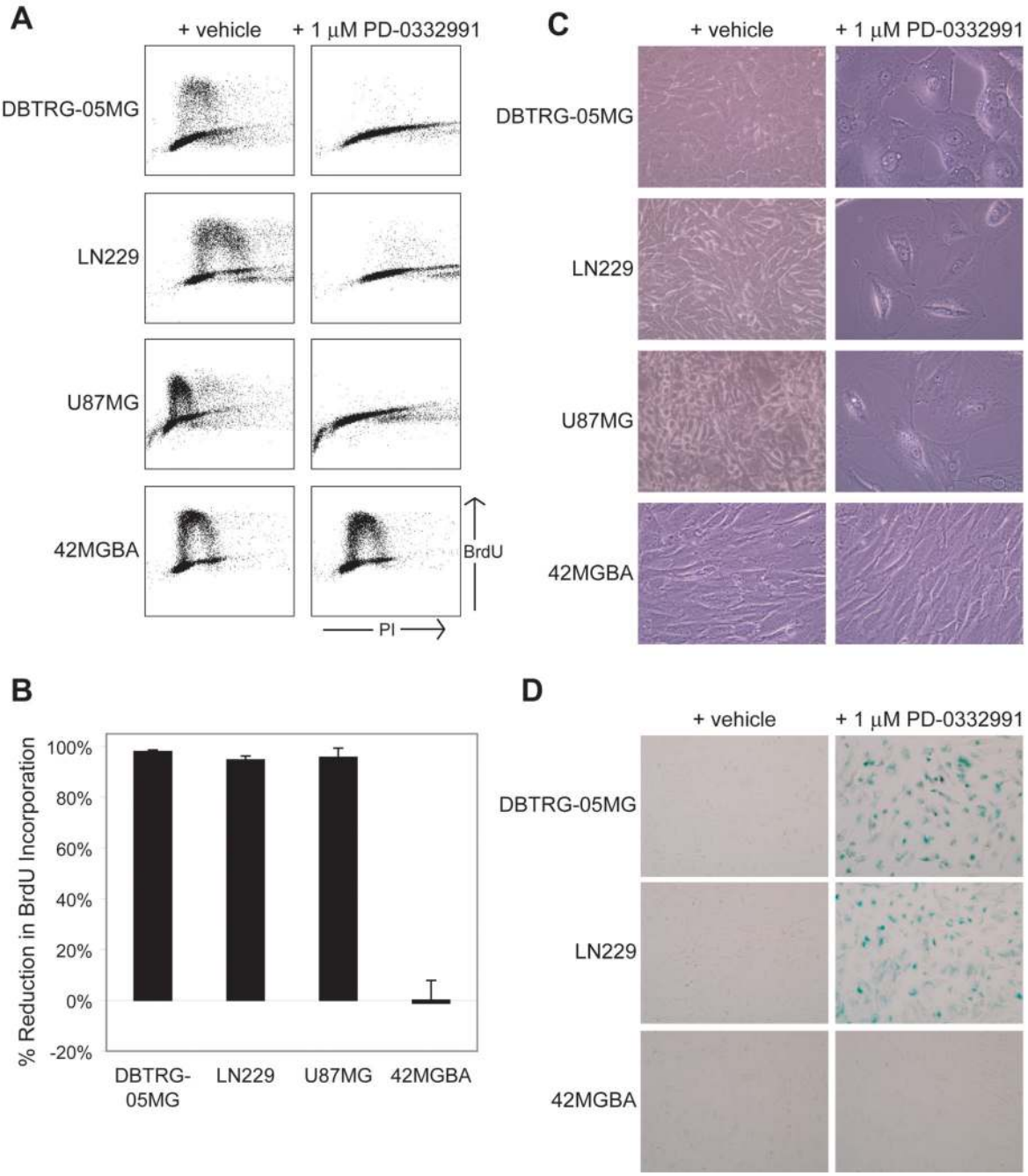

Figure 1.

PD-0332991 induces cell cycle arrest and senescence of GBM cells dependent on Rb status. *A*, Flow cytometry analysis of three Rb-proficient GBM cell lines (DBTRG-05MG, LN229, and U87MG) and one Rb-deficient cell line (42MGBA) following culture in the presence of vehicle or 1 μM PD-0332991 for 48 hrs and then pulsed with BrdU for 1 hr. Cell cycle distribution plots of BrdU vs. propidium iodide (PI) intensity are shown. *B*, Quantification of reduction in S phase cells depicted in *A*. *C*, Photomicrographs of the Rb-proficient cell lines after culture in the presence of 1 μM PD-0332991 for 7 days reveal growth inhibition and morphological changes resembling cellular senescence, whereas the Rb-deficient cell line (42MGBA) shows no growth inhibition or morphological changes. *D*, Staining for

senescence-associated β-galactosidase activity in two Rb-proficient cell lines and one Rb-deficient cell line after culture in the presence of vehicle or 1 μM PD-0332991 for 2 weeks.

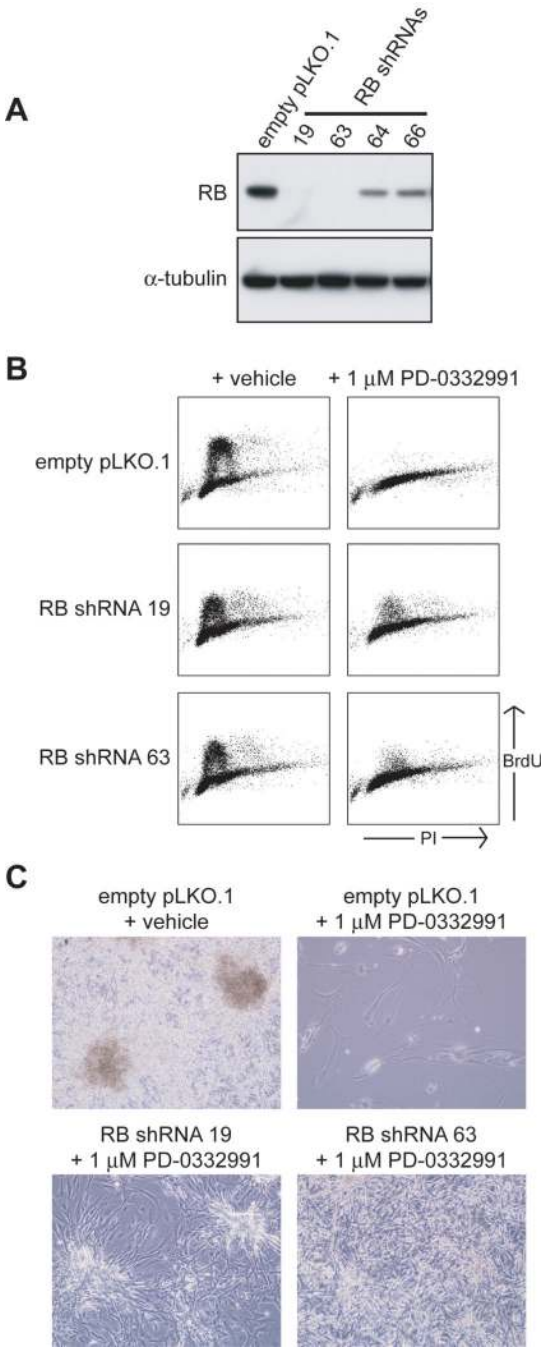

Figure 2.

Depletion of Rb expression alleviates growth arrest induced by PD-0332991. *A*, Five unique shRNAs to RB1 were transduced into U87MG cells, and total protein from stably expressing clones was resolved by SDS-PAGE and immunoblotted with an Rb antibody. Clones 19 and 63 show greater than 99% knockdown of Rb expression relative to the empty pLKO.1-infected clone. *B*, Flow cytometry analysis following a 1 hr BrdU pulse of U87MG Rb shRNA clones 19 and 63 after 48 hrs of treatment with vehicle or 1 μM PD-0332991. *C*, Photomicrographs of clones 19 and 63 following incubation with 1 μM PD-0332991 for 3 weeks demonstrates their failure to arrest and eventual growth to confluence in spite of sustained incubation with the cdk4/6 inhibitor.

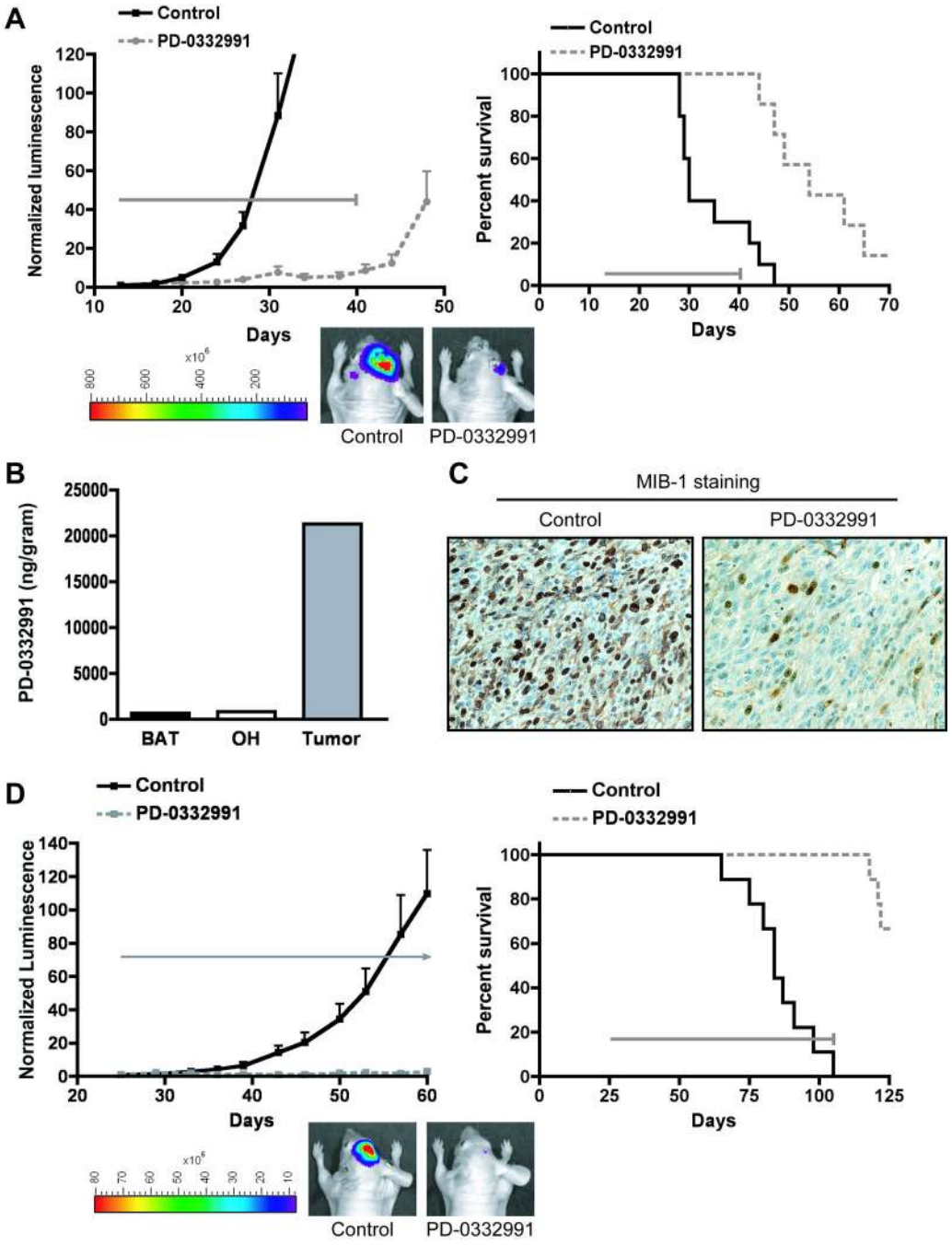

Figure 3.

PD-0332991 crosses the blood-brain barrier and potently suppresses the growth of intracranial human GBM xenografts. U87MG cells (*A*–*C*) and primary xenograft GBM 39 (*D*) were modified to express luciferase and injected into the brains of nude mice to establish intracranial tumors. Mice were randomized to control (vehicle treated) and PD-0332991 treatment groups, with PD-0332991 administered daily by oral gavage at 150 mg/kg (4 weeks for U87MG; 12 weeks for GBM 39: see gray horizontal arrows in *A*,*D*). Mice were imaged 1–2× weekly for bioluminescence intensity (see examples in *A* and *D*), with luminescence values of individual mice normalized to their corresponding luminescence at the start of therapy, and mean normalized values plotted (left panels of *A*,*D*). *B*, One mouse

from the U87MG treatment group was euthanized and its brain was dissected for the isolation of pure tumor, brain adjacent to tumor (BAT), and normal tissue from the opposite hemisphere (OH). These specimens were analyzed by LC-MS/MS for determination o f P D-0332991 content which demonstrated dissemination of PD-0332991 into the brain and accumulation in tumor tissue. *C*, One mouse from the U87MG treatment group and one mouse from the control group were euthanized on the same day post tumor cell injection, and their brains dissected, fixed, and embedded in paraffin. Immunohistochemistry with MIB-1 antibody revealed >8-fold reduction in MIB-1 index in the tumor from the PD-0332991 treated mouse relative to the control. *A*,*D (right panels)* Kaplan-Meier survival plots for the U87MG and GBM 39 experiments demonstrating significant survival benefit from PD-0332991 treatment ($p < 0.001$ in each case). See Supplemental Table 2 for statistical analysis of mean survival.

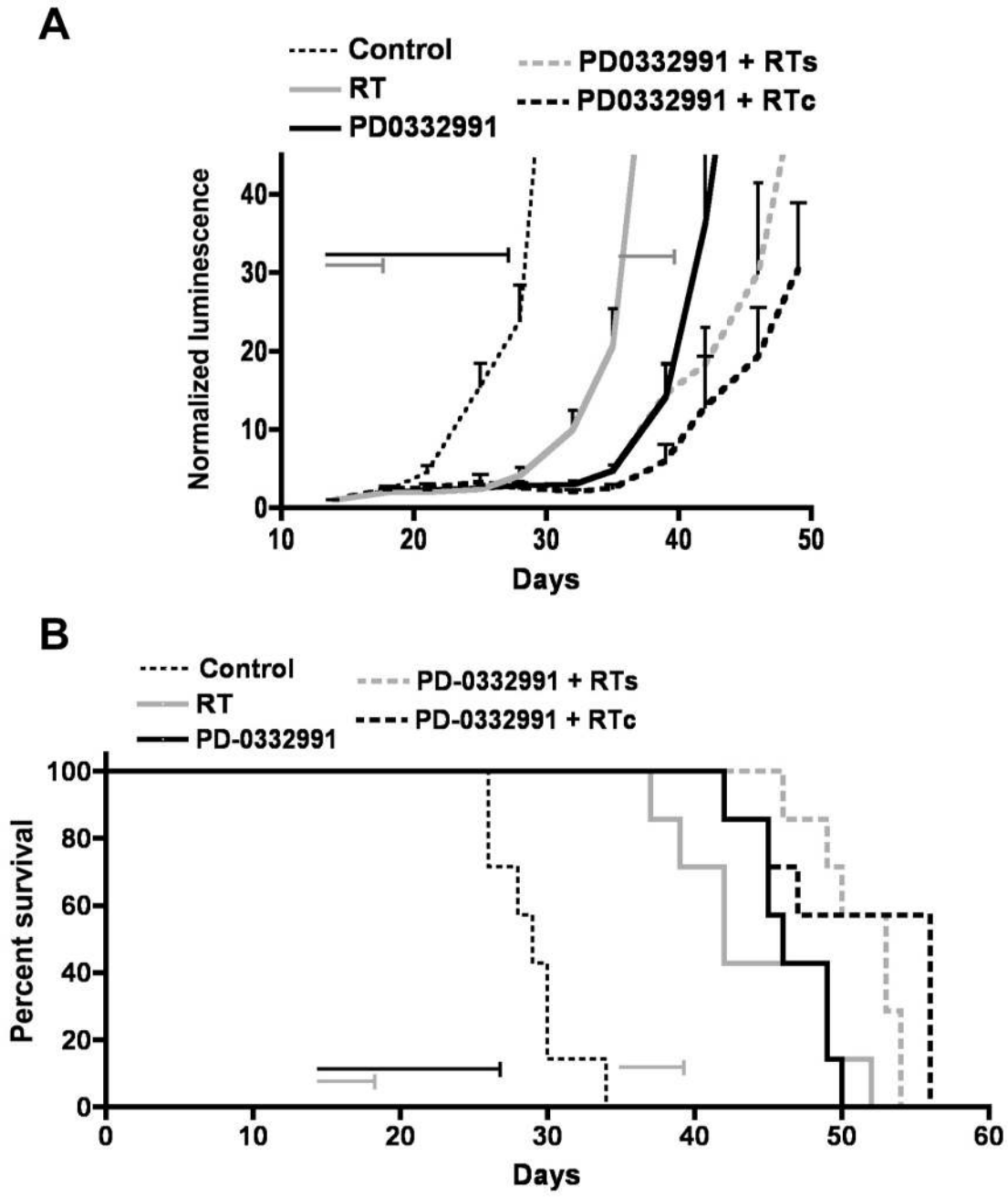

Figure 4.

PD-0332991 combined with radiation therapy shows enhanced anti-tumor activity and extends survival. Luciferase-modified U87MG cells were injected into the brains of nude mice to establish intracranial tumors. Mice were randomized to four treatment groups: untreated (Control), radiation only (RT, 2 Gy/day ×5 days, horizontal gray arrow), PD-0332991 only (150 mg/kg/day × 14 days, horizontal black arrow), PD-0332991 and concurrent radiation (RTc), and PD-0332991 with subsequent radiation (RTs). *A*, Bioluminescence monitoring was conducted 1–2× weekly throughout the course of the experiment, with mean normalized values plotted for each treatment group. *B*, Kaplan-Meier

survival plots demonstrating survival benefit from PD-0332991 and radiation combination therapy. See Supplemental Table 2 for statistical analysis of mean survival.

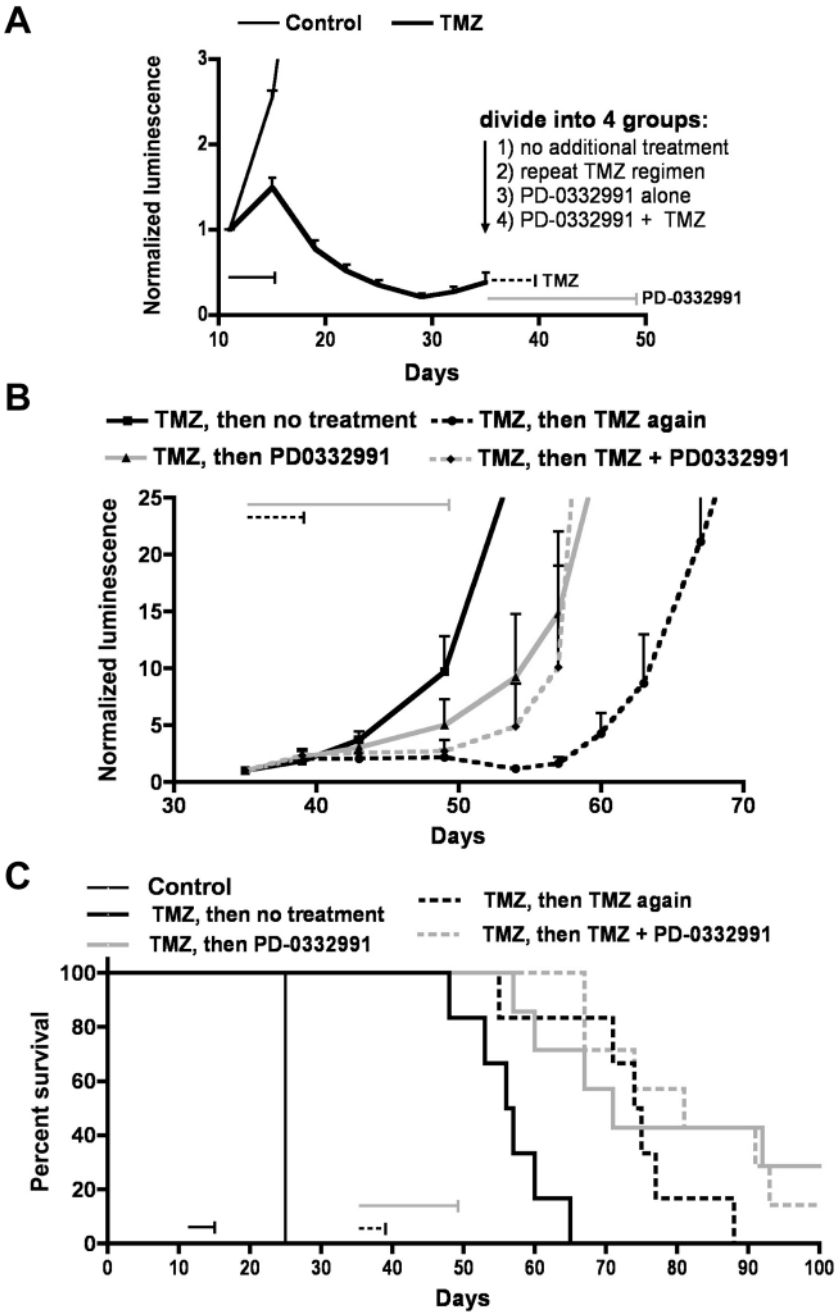

Figure 5.

Evaluation of PD-0332991 activity against intracranial GBM xenografts that have recurred following initial treatment with temozolomide. *A*, Luciferase-modified U87MG cells were injected into the brains of athymic mice. Mice with proliferating tumors were randomized into untreated (Control) and temozolomide treated groups (TMZ, 10 mg/kg/day for 5 days). *B*, When successive mean normalized luminescence values indicated tumor recurrence of TMZ treated mice (day 35), these mice were randomized to 4 treatment groups: no additional treatment, repeat treatment with the same TMZ regimen, treatment with PD-0332991 (150 mg/kg/day for 14 days), or combined TMZ + PD-0332991 treatment, and then monitored for bioluminescent intensity 1–2× weekly during therapy. *C*, Kaplan-Meier

survival plots demonstrating significant survival benefit from PD-0332991 therapy of recurrent tumors. See Supplemental Table 2 for statistical analysis of mean survival.

Table 1

Genetic lesions of the cdk4/6-cyclin D-INK4-Rb signaling pathway and *in vitro* sensitivity to PD-0332991 for a panel of 21 GBM cell lines.

	sensitivity to 1 μM PD-0332991[†]	Genetic lesions present in cells[‡]							
cell line		**RB1**	**CDKN2A/B**	**CDKN2C**	**CDK4***	**CDK6***	**CCND1***	**CCND2***	**CCND3***
8MGBA	−	HD							
42MGBA	−	no protein *	HD						
A172	+++		HD						
AM-38	++		HD						
CCF-STTG1	+++					AMP			AMP
DBTRG-05MG	+++		HD						
DKMG	+++		HD						
GAMG	+		HD						
GMS10	−	MUT (nonsense)							
H4	+		HD						
Hs683	+++	*	HD						
KG-1-C	+++	*	HD						
LN18	+	*	HD						
LN229	+++	*	HD	HD					
LN405	−	MUT (nonsense)							
M059J	−	MUT (splice site)							
NMC-G1	+++		HD						
SNB19	+++		HD	HD					
T98G	+		HD	HD					
U138MG	+++		HD						
U87MG	+++		HD	HD					
Total events	**16**	**5**	**16**	**4**	**0**	**1**	**0**	**0**	**1**
Frequency	**76%**	**24%**	**76%**	**19%**	**0%**	**5%**	**0%**	**0%**	**5%**

[†]A panel of 21 GBM cell lines was grown *in vitro* in the presence of vehicle or 1 μM PD-0332991 for 48 hrs, pulsed with BrdU for 1 hr, then fixed and stained with propidium iodide and FITC-conjugated BrdU antibody for flow cytometry analysis (see Supplemental Fig. 2). A sensitivity score of +++ was assigned to cells with greater than 95% reduction in BrdU incorporation after treatment with 1 μM PD-0332991 compared to vehicle, ++ for 75–95% reduction, + for 10–75% reduction, and − for less than 10% reduction.

[‡] Genetic data are derived from exonic sequencing and Affymetrix 250K SNP arrays performed by Solomon *et al.* (7,21,22) and from Affymetrix 6.0 SNP arrays and the COSMIC database of the Cancer Genome Project of the Wellcome Trust Sanger Institute (http://www.sanger.ac.uk/genetics/CGP/). HD, homozygous deletion; MUT, homozygous mutation; AMP, genomic amplification;

[*] mutation status of gene not determined.